Simplified Finite Control Set-Model Predictive Control for Matrix Converter-Fed PMSM Drives

Mohsen Siami, Davood Arab Khaburi, and Jose Rodriguez, *Fellow, IEEE*

***Abstract*—Finite control set-model predictive control (FCS-MPC) is emerging as an attractive alternative for power converters control. In comparison with the classical linear controllers, FCS-MPC needs a shorter control loop cycle time to achieve the same performance. But, the conventional FCS-MPC involves a large amount of calculation. The calculation efforts increase with the number of switching states of the power converter as well as the control objectives, which is a challenge for its application. This paper proposes an effective method to simplify the FCS-MPC and to reduce its calculation efforts for its application in matrix converter-fed permanent magnet synchronous motors. The experimental results which verify the good performance of the proposed method are presented.**

***Index Terms*—Matrix converter, permanent magnet motor, predictive control.**

I. Introduction

MATRIX converters are attracting wide attention because of their interesting features such as compact design, bidirectional power flow, controllable input reactive power, and sinusoidal input/output currents [1]. Since Alesina and Venturini introduced the first modulation method, known as direct transfer function modulation [2], different modulation methods and control strategies for matrix converters have been proposed in the literature including the scalar method, pulse with modulation and space vector modulation techniques, direct torque control, and predictive control [3].

The finite control set-model predictive control (FCS-MPC) is the most attractive kind of predictive control and has been developed widely in recent years due to its intuitive concept, straightforward implementation, and easy inclusion of system constraints [4]–[9]. In FCS-MPC, the control objectives are predicted for all of possible switching states of the power converter and the optimal state is selected through the minimization of a cost function. So, the output of control algorithm is only one switching state in every control interval and no modulation stage is required. Thus, its switching frequency is variable and to achieve the similar performance of the modulation-based control strategies, a shorter control time interval is required [10], [11]. However, the calculation time for prediction and evaluation of all switching states is an obstacle to shorten the control time interval. The calculation time is more challenging when the number of switching states of the power converter increases or more objectives are considered for control. For example, in the case of a three-phase to three-phase matrix converter, there are 27 admissible switching states and the calculation time increases rapidly with more control objectives. Hence, the implementation of FCS-MPC for a matrix converter requires powerful hardware that limits its use in industry applications [12]–[21].

In recent years, different strategies have been proposed to decrease the computational burden in FCS-MPC [22]–[31]. In [22] and [23], the calculation effort for long prediction horizons decreased through discarding suboptimal sequences by adopting branch and bound algorithm. In [24], the approximate dynamic programming is used to estimate the infinite horizon tail cost of the MPC problem formulation which decreases the horizon length and reduces the computational burden. Sector distribution on input voltage vector is used in [25] to decrease the number of candidate voltage vectors for prediction. There are several other approaches to reduce the computational burden such as double-vector-based approach [26], selecting a subset of adjacent vectors [27] graphical algorithm [28], and modified switching algorithm [29]. A lookup table has been proposed in [30] to decrease the number of candidate vectors for predictive control of an induction machine fed by a two-level inverter, where the control objectives are only the motor torque and flux and the designing of the cost function is relatively easy. Similar idea has been proposed in [31] for matrix converter. In [32]–[34], interesting approaches have been suggested to decrease the running time of FCS-MPC. The main idea in these papers is similar, where the optimum switching state is decided based on the desired voltage vectors. The control objectives are load currents in [32], motor torque and flux in [33], and reactive and active powers in [34]. These techniques have been applied through a two-level inverter, a three-level inverter, and a doubly fed induction generator, respectively.

The main contribution of this paper is to simplify the implementation of FCS-MPC on a matrix converter-fed permanent magnet synchronous motor (PMSM) by extending the introduced ideas in [32]–[34]. This simplification is achieved through two main steps: 1) elimination of the prediction of

Manuscript received December 20, 2016; revised March 12, 2017; accepted April 11, 2017. Date of publication April 24, 2017; date of current version December 1, 2017. This work was supported by the Fondecyt and CONICYT-Basal Project FB0008. Recommended for publication by Associate Editor Y. Abdel-Rady I. Mohamed. *(Corresponding author: Davood Arab Khaburi.)*

M. Siami and D. Arab Khaburi are with the Center of Excellence for Power Systems Automation and Operation, Department of Electrical Engineering, Iran University of Science and Technology, Tehran 1311416846, Iran (e-mail: siami@iust.ac.ir; khaburi@iust.ac.ir).

J. Rodríguez is with the Faculty of Engineering, Universidad Andres Bello, Santiago 001, Chile (e-mail: jose.rodriguez@unab.cl).

Color versions of one or more of the figures in this paper are available online at http://ieeexplore.ieee.org.

Digital Object Identifier 10.1109/TPEL.2017.2696902

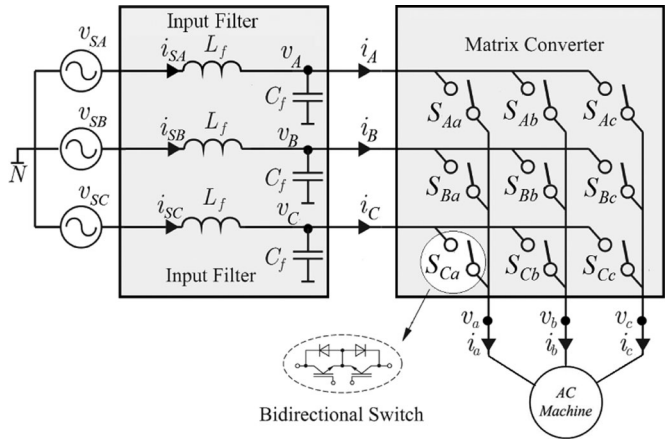

Fig. 1. Matrix converter and power circuit.

motor currents for different switching states; and 2) reduction of candidate switching state for prediction and evaluation. The experimental implementations of the proposed method and the conventional FCS-MPC show that with the proposed method the running time is considerably reduced without significant effect on the control performance.

II. System Model

The system studied in this paper comprising matrix converter, input filter, and PMSM is presented in Fig. 1. The input current and the output voltage space vectors of matrix converter are given, respectively, as

$$\mathbf{i}_i = \frac{2}{3}\left(i_A + a\cdot i_B + a^2\cdot i_C\right) = i_{i\max}\cdot e^{j\beta_i} \tag{1}$$

$$\mathbf{v}_o = \frac{2}{3}\left(v_a + a\cdot v_b + a^2\cdot v_c\right) = v_{o\max}\cdot e^{j\alpha_o} \tag{2}$$

where $a = e^{j(2\pi/3)}$ and i_a, i_b, and i_c are input phase currents and v_a, v_b, and v_c are output phase voltages of the matrix converter. $i_{i\max}$ and $v_{o\max}$ are the amplitudes of input current and output voltage vectors, respectively, and β_i and α_o are the angles of input current and output voltage vectors, respectively. Similar definitions can be expressed for the source voltage vector $\mathbf{v}_s$, the source current vector $\mathbf{i}_s$, and the output current vector $\mathbf{i}_o$.

The relationship between the input and output voltages of matrix converter can be given by

$$v_o = \begin{bmatrix} v_a \\ v_b \\ v_c \end{bmatrix} = \begin{bmatrix} S_{\mathrm{Aa}} & S_{\mathrm{Ba}} & S_{\mathrm{Ca}} \\ S_{\mathrm{Ab}} & S_{\mathrm{Bb}} & S_{\mathrm{Cb}} \\ S_{\mathrm{Ac}} & S_{\mathrm{Bc}} & S_{\mathrm{Cc}} \end{bmatrix} \cdot \begin{bmatrix} v_A \\ v_B \\ v_C \end{bmatrix} = S\cdot v_i. \tag{3}$$

And the relationship between the input and output currents of matrix converter can be given by

$$i_i = \begin{bmatrix} i_A \\ i_B \\ i_C \end{bmatrix} = \begin{bmatrix} S_{\mathrm{Aa}} & S_{\mathrm{Ab}} & S_{\mathrm{Ac}} \\ S_{\mathrm{Ba}} & S_{\mathrm{Bb}} & S_{\mathrm{Bc}} \\ S_{\mathrm{Ca}} & S_{\mathrm{Cb}} & S_{\mathrm{Cc}} \end{bmatrix} \cdot \begin{bmatrix} i_a \\ i_b \\ i_c \end{bmatrix} = S^T\cdot i_o \tag{4}$$

where S^T is the transpose of matrix S and S_{xy} with $x \in \{A, B, C\}$ and $y \in \{a, b, c\}$ is the switching function of a bidirectional switch as

$$S_{\mathrm{xy}} = \begin{cases} 0 & \text{if } S_{\mathrm{xy}} \text{ is open} \\ 1 & \text{if } S_{\mathrm{xy}} \text{ is close} \end{cases}. \tag{5}$$

TABLE I
Space Vectors of a Three-Phase to Three-Phase Matrix Converter

State	On Switches			v_o	α_o	i_i	β_i
$+1$	$S_{\mathrm{A\,a}}$	$S_{\mathrm{B\,b}}$	$S_{\mathrm{B\,c}}$	$2/3v_{\mathrm{A\,B}}$	0	$2/\sqrt{3}i_a$	$-\pi/6$
-2	$S_{\mathrm{B\,a}}$	$S_{\mathrm{A\,b}}$	$S_{\mathrm{A\,c}}$	$-2/3v_{\mathrm{A\,B}}$	0	$-2/\sqrt{3}i_{\mathrm{a}}$	$-\pi/6$
$+2$	$S_{\mathrm{B\,a}}$	$S_{\mathrm{C\,b}}$	$S_{\mathrm{C\,c}}$	$2/3v_{\mathrm{B\,C}}$	0	$2/\sqrt{3}i_{\mathrm{a}}$	$\pi/2$
-2	$S_{\mathrm{C\,a}}$	$S_{\mathrm{B\,b}}$	$S_{\mathrm{B\,c}}$	$-2/3v_{\mathrm{B\,C}}$	0	$-2/\sqrt{3}i_{\mathrm{a}}$	$\pi/2$
$+3$	$S_{\mathrm{C\,a}}$	$S_{\mathrm{A\,b}}$	$S_{\mathrm{A\,c}}$	$2/3v_{\mathrm{C\,a}}$	0	$2/\sqrt{3}i_{\mathrm{a}}$	$7\pi/6$
-3	$S_{\mathrm{A\,a}}$	$S_{\mathrm{C\,b}}$	$S_{\mathrm{C\,c}}$	$-2/3v_{\mathrm{C\,a}}$	0	$-2/\sqrt{3}i_{\mathrm{a}}$	$7\pi/6$
$+4$	$S_{\mathrm{B\,a}}$	$S_{\mathrm{A\,b}}$	$S_{\mathrm{B\,c}}$	$2/3v_{\mathrm{A\,B}}$	$2\pi/3$	$2/\sqrt{3}i_b$	$-\pi/6$
-4	$S_{\mathrm{A\,a}}$	$S_{\mathrm{B\,b}}$	$S_{\mathrm{A\,c}}$	$-2/3v_{\mathrm{A\,B}}$	$2\pi/3$	$-2/\sqrt{3}i_{\mathrm{b}}$	$-\pi/6$
$+5$	$S_{\mathrm{C\,a}}$	$S_{\mathrm{B\,b}}$	$S_{\mathrm{C\,c}}$	$2/3v_{\mathrm{B\,C}}$	$2\pi/3$	$2/\sqrt{3}i_{\mathrm{b}}$	$\pi/2$
-5	$S_{\mathrm{B\,a}}$	$S_{\mathrm{C\,b}}$	$S_{\mathrm{B\,c}}$	$-2/3v_{\mathrm{B\,C}}$	$2\pi/3$	$-2/\sqrt{3}i_{\mathrm{b}}$	$\pi/2$
$+6$	$S_{\mathrm{A\,a}}$	$S_{\mathrm{C\,b}}$	$S_{\mathrm{A\,a}}$	$2/3v_{\mathrm{C\,A}}$	$2\pi/3$	$2/\sqrt{3}i_{\mathrm{b}}$	$7\pi/6$
-6	$S_{\mathrm{C\,a}}$	$S_{\mathrm{A\,b}}$	$S_{\mathrm{C\,c}}$	$-2/3v_{\mathrm{C\,A}}$	$2\pi/3$	$-2/\sqrt{3}i_{\mathrm{b}}$	$7\pi/6$
$+7$	$S_{\mathrm{B\,a}}$	$S_{\mathrm{B\,b}}$	$S_{\mathrm{A\,c}}$	$2/3v_{\mathrm{A\,B}}$	$4\pi/3$	$2/\sqrt{3}i_c$	$-\pi/6$
-7	$S_{\mathrm{A\,a}}$	$S_{\mathrm{A\,b}}$	$S_{\mathrm{B\,c}}$	$-2/3v_{\mathrm{A\,B}}$	$4\pi/3$	$-2/\sqrt{3}i_{\mathrm{c}}$	$-\pi/6$
$+8$	$S_{\mathrm{C\,a}}$	$S_{\mathrm{B\,b}}$	$S_{\mathrm{C\,c}}$	$2/3v_{\mathrm{B\,C}}$	$4\pi/3$	$2/\sqrt{3}i_{\mathrm{c}}$	$\pi/2$
-8	$S_{\mathrm{B\,a}}$	$S_{\mathrm{B\,b}}$	$S_{\mathrm{C\,c}}$	$-2/3v_{\mathrm{B\,C}}$	$4\pi/3$	$-2/\sqrt{3}i_{\mathrm{c}}$	$\pi/2$
$+9$	$S_{\mathrm{A\,a}}$	$S_{\mathrm{A\,b}}$	$S_{\mathrm{C\,c}}$	$2/3v_{\mathrm{C\,A}}$	$4\pi/3$	$2/\sqrt{3}i_{\mathrm{c}}$	$7\pi/6$
-9	$S_{\mathrm{C\,a}}$	$S_{\mathrm{C\,b}}$	$S_{\mathrm{C\,c}}$	$-2/3v_{\mathrm{C\,A}}$	$4\pi/3$	$-2/\sqrt{3}i_{\mathrm{c}}$	$7\pi/6$
0_a	$S_{\mathrm{A\,a}}$	$S_{\mathrm{A\,b}}$	$S_{\mathrm{A\,c}}$	0	–	0	–
0_b	$S_{\mathrm{B\,a}}$	$S_{\mathrm{B\,b}}$	$S_{\mathrm{B\,c}}$	0	–	0	–
0_c	$S_{\mathrm{C\,a}}$	$S_{\mathrm{C\,b}}$	$S_{\mathrm{C\,c}}$	0	–	0	–
$+10$	$S_{\mathrm{A\,a}}$	$S_{\mathrm{B\,b}}$	$S_{\mathrm{C\,c}}$	$v_{i\max}$	α_{i}	$i_{\mathrm{o\,max}}$	β_{o}
-10	$S_{\mathrm{A\,a}}$	$S_{\mathrm{C\,b}}$	$S_{\mathrm{B\,c}}$	$v_{i\max}$	$-\alpha_{\mathrm{i}}$	$i_{\mathrm{o\,max}}$	$-\beta_{\mathrm{o}}$
$+11$	$S_{\mathrm{C\,a}}$	$S_{\mathrm{A\,b}}$	$S_{\mathrm{B\,c}}$	$v_{i\max}$	$\alpha_{\mathrm{i}}+2\pi/3$	$i_{\mathrm{o\,max}}$	$\beta_{\mathrm{o}}+2\pi/3$
-11	$S_{\mathrm{B\,a}}$	$S_{\mathrm{A\,b}}$	$S_{\mathrm{C\,c}}$	$v_{i\max}$	$-\alpha_{\mathrm{i}}+2\pi/3$	$i_{\mathrm{o\,max}}$	$-\beta_{\mathrm{o}}+2\pi/3$
$+12$	$S_{\mathrm{B\,a}}$	$S_{\mathrm{C\,b}}$	$S_{\mathrm{A\,c}}$	$v_{i\max}$	$\alpha_{\mathrm{i}}+4\pi/3$	$i_{\mathrm{o\,max}}$	$\beta_{\mathrm{o}}+4\pi/3$
-12	$S_{\mathrm{C\,a}}$	$S_{\mathrm{B\,b}}$	$S_{\mathrm{A\,c}}$	$v_{i\max}$	$-\alpha_{\mathrm{i}}+4\pi/3$	$i_{\mathrm{o\,max}}$	$-\beta_{\mathrm{o}}+4\pi/3$

Since the input side of matrix converter is a voltage source in Fig. 1, the short circuit in the input side is not allowed and due to inductive nature of the load (PMSM), the output side current should not be interrupted. Avoiding these conditions, there are 27 allowable switching states for the matrix converter. These states and their associated output-voltage and input-current vectors are presented in Table I. The switching states can be classified into three groups, comprising "active vectors" with variable magnitude and fixed direction (±1 to ±9), "rotating vectors" with fixed magnitude and variable direction (±10 to ±12), and "zero vectors" with zero magnitude (0*a*–0*c*).

III. Conventional FCS-MPC for a Matrix Converter-Fed PMSM

The conventional FCS-MPC involves two main steps: 1) predicting control variables for all admissible switching states of the converter; and 2) evaluating the predicted values in a cost function and determining the state that minimizes the cost function. In this paper, we consider the stator currents of PMSM and the input reactive power of matrix converter as control variables to analyze the performance and required computational efforts of the conventional FCS-MPC.

The dynamic equation of a surface-mounted PMSM in the stationary reference frame is

$$L_s \frac{d\mathbf{i}_o}{dt} = -R_s \mathbf{i}_o - \mathbf{e} + \mathbf{v}_o \tag{6}$$

where R_s and L_s are the stator resistance and stator inductance, respectively, and $\mathbf{e}$ is the back electromotive force (EMF) vector.

To predict the stator currents, the forward Euler discretization is applied to (6), and the discrete-time expression of (6) with sampling time T_s is obtained as

$$\mathbf{i}_{o|\mathrm{sw}}(k+1) = \mathbf{i}_o(k) + \frac{T_s}{L_s}[-R_s \mathbf{i}_o(k) - \mathbf{e}(k) + \mathbf{v}_{o|\mathrm{sw}}] \tag{7}$$

where "sw" indicates different switching states of the matrix converter. The magnitude and phase of output voltage vectors associated with different switching states are listed in Table I. Equation (7) states the motor current at instant $(k+1)$ is determined by the back EMF and current at instant $(k+1)$, denoted with $\mathbf{e}(k)$, $\mathbf{i}_o(k)$, respectively, and the output voltage of matrix converter, denoted with $\mathbf{v}_o$.

For predicting the input reactive power, a discrete-time model is derived from continuous-time model of the input filter. The input filter's model, shown in Fig. 1, can be represented by the following continuous-time space-state model:

$$\begin{bmatrix} \dot{\mathbf{v}}_i \\ \dot{\mathbf{i}}_s \end{bmatrix} = A \begin{bmatrix} \mathbf{v}_i \\ \mathbf{i}_s \end{bmatrix} + B \begin{bmatrix} \mathbf{v}_s \\ \mathbf{i}_i \end{bmatrix} \tag{8}$$

where

$$A = \begin{bmatrix} 0 & \dfrac{1}{C_f} \\ \dfrac{-1}{L_f} & \dfrac{-R_f}{L_f} \end{bmatrix}, \quad B = \begin{bmatrix} 0 & \dfrac{-1}{C_f} \\ \dfrac{1}{L_f} & 0 \end{bmatrix} \tag{9}$$

where C_f and L_f are the filter capacitance and inductance, respectively, and R_f is the leakage resistance of L_f. The discrete-time state-space model of the input filter can be derived from (9) as follows:

$$\begin{bmatrix} \mathbf{v}_i(k+1) \\ \mathbf{i}_s(k+1) \end{bmatrix} = A_d \begin{bmatrix} \mathbf{v}_i(k) \\ \mathbf{i}_s(k) \end{bmatrix} + B_d \begin{bmatrix} \mathbf{v}_s(k) \\ \mathbf{i}_i(k) \end{bmatrix} \tag{10}$$

where

$$A_d = e^{AT_s}, \quad B_d = \int_0^{T_s} e^{A(T_s-\tau)} B d\tau\,. \tag{11}$$

The source current is predicted by solving $\mathbf{i}_s\,(k+1)$ from (10) as

$$\begin{aligned} \mathbf{i}_{s|\mathrm{sw}}(k+1) = {} & A_d(2,1)\mathbf{v}_i(k) + A_d(2,2)\mathbf{i}_s(k) \\ & + B_d(2,1)\mathbf{v}_s(k) + B_d(2,2)\mathbf{i}_{i|\mathrm{sw}}. \end{aligned} \tag{12}$$

Equation (13) states the source current at instant $(k+1)$ is determined by the source voltage, source current, and the input voltage of matrix converter at instant (k), denoted with $\mathbf{v}_s$, $\mathbf{i}_s$, and $\mathbf{v}_i$, respectively, and the input current of matrix converter denoted with $\mathbf{i}_i$. $\mathbf{v}_s$, $\mathbf{i}_s$, and $\mathbf{v}_i$ are given by measuring and the input current of the matrix converter $\mathbf{i}_i$ is calculated using (2) and (4) for each switching state.

The instantaneous input reactive power is predicted by

$$Q_{\mathrm{sw}}(k+1) = \mathrm{Im}\left\{\mathbf{v}_s(k+1) \cdot \bar{\mathbf{i}}_{s|\mathrm{sw}}(k+1)\right\} \tag{13}$$

where $\bar{\mathbf{i}}_s$ is the complex conjugate of vector $\mathbf{i}_s$. Since the source voltages are low-frequency signals, it can be assumed that $\mathbf{v}_s(k+1) \approx \mathbf{v}_s(k)$.

Equations (7) and (13) are applied to predict the motor current and the input reactive power at instant $(k+1)$ for all admissible switching states of the matrix converter, supposing the application of each switching state from instant k to instant $k+1$. A cost function is required to decide the best switching state. A classical cost function can be defined as the absolute error between the predicted values and their corresponding reference values as

$$\mathrm{CF}_{\mathrm{sw}} = \left|\mathbf{i}_o^* - \mathbf{i}_{o|\mathrm{sw}}(k+1)\right| + k_Q \left|Q^* - Q_{\mathrm{sw}}(k+1)\right| \tag{14}$$

where $\mathbf{i}_o^*$ and Q^* are the reference values of motor current and input reactive power, respectively. k_Q is a weighting factor which handles the relative importance of reactive power over motor current. An interesting idea has been proposed in [35] and [36] to discard the weighting factor. But, the implementation of this idea for a matrix converter with 27 possible switching states requires a lot of calculations.

The realization of conventional FCS-MPC is to find the switching state that minimizes the cost function (14) and then applies it to the converter. Since there are three switching states that produce zero vectors ($0a$, $0b$, $0c$), the 27 admissible switching states of the matrix converter produce 25 different combinations of output voltage and input current vectors. In conclusion, a conventional FCS-MPC of matrix converter requires 25 motor current calculations, 25 input reactive power calculations, and 25 calculations of the cost function. These calculations are computationally expensive and need powerful hardware and low sampling frequency. This shortcoming restricts the industrial application of FCS-MPC for matrix converters.

IV. Simplified FCS-MPC for a Matrix Converter-Fed PMSM

A. Simplification of Prediction

The key point of the proposed method to simplify FCS-MPC is to avoid 25 motor current predictions for instant $k+1$. Instead, it uses desired output voltage vector for prediction procedure.

The desired output voltage vector $\boldsymbol{v}_o{}^*(k)$ to achieve the motor reference current at instant $k+1$ can be obtained from (7) as

$$\mathbf{v}_o^*(k) = \frac{L_s}{T_s}[\mathbf{i}_o^*(k+1) - \mathbf{i}_o(k)] + R_s \mathbf{i}_o(k) + \mathbf{e}(k). \tag{15}$$

Equation (15) states the motor current will be exactly equal to its reference at instant $k+1$, if the exerted voltage vector to the motor through the converter at instant k can be the same as $\boldsymbol{v}_o{}^*(k)$, calculated with (15). But, due to lack of any modulator, the matrix converter can produce only 25 voltage vectors that may not be exactly equal to desired voltage vector. However, exerting the nearest voltage vector to the desired voltage vector

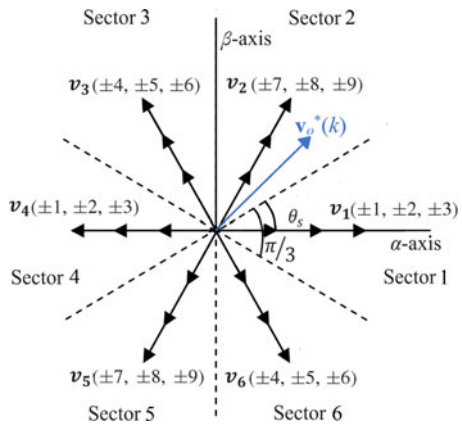

Fig. 2. Active voltage vectors of a matrix converter.

is the most appropriate choice to reduce the error between the stator current and its reference at the end of the next sampling time. For this purpose, a new cost function can be defined as follows:

$$\mathrm{CF}_{\mathrm{sw}} = \left|\mathbf{v}_o^*(k) - \mathbf{v}_{o|\mathrm{sw}}\right|. \tag{16}$$

To control the input reactive power a second term is added to the cost function (16). To do this, (16) is extended to

$$\mathrm{CF}_{\mathrm{sw}} = \left|\mathbf{v}_o^*(k) - \mathbf{v}_{o|\mathrm{sw}}\right| + k_Q \left|Q^* - Q_{\mathrm{sw}}(k+1)\right|. \tag{17}$$

The cost function (17) can be calculated for all 25 switching states of the matrix converter and the one that minimizes it is applied to the converter. In this way, the calculations of 25 motor current predictions are avoided and only one prediction is required to calculate the desired voltage vector.

B. Reducing the Candidate Switching State for Prediction

The proposed method can be further simplified by reducing the candidate switching state for prediction and evaluation in the cost function.

Fig. 2 depicts the space distribution of active voltage vectors of the matrix converter in α–β plane. As depicted, the matrix converter generates 18 active vectors $\{\pm 1, \ldots, \pm 9\}$ in six different directions $v_1, \ldots, v_6$. The direction of each vector is constant but its magnitude is dependent on the instant value of the input voltages of the matrix converter. The α–β plane can be divided into six sectors $S_1, \ldots, S_6$ where

$$(2N-1)\pi/6 \leq S_N \leq (2N+1)\pi/6. \tag{18}$$

According to the sector which the desired output voltage vector $\mathbf{v}_o^*(k)$ is located, the active vectors located in corresponding sector are the closest vectors to $\mathbf{v}_o^*(k)$. For example, supposing that $\mathbf{v}_o^*(k)$ is located in sector 2, the active vectors in the same direction with v_2 are the closest vectors to $\mathbf{v}_o^*(k)$. On the other hand, for each direction $v_1, \ldots, v_6$, matrix converter can generate three active vectors with different amplitudes. According to [37], at least one of these vectors reduces the input reactive power and one of them increases it. So, these three active vectors can ensure the possible demand for decrease or increase of input reactive power. In addition to these three active vectors, there are six rotating vectors whose directions are not fixed and may be close to $\mathbf{v}_o^*(k)$. Therefore, these six rotating vectors along with the three active vectors and one proper zero vector can be selected as candidate vectors for prediction and evaluation.

In conclusion, in the proposed method not only the 25 motor current predictions are eliminated, but also the 25 input reactive power predictions and 25 cost function evaluations which are required in conventional FCS-MPC are reduced to 10 input reactive power predictions and 10 cost function evaluations. In this way, the running time of the algorithm is considerably reduced.

TABLE II
PROPER DIRECTION OF ACTIVE VECTORS ACCORDING THE SECTOR THAT THE DESIRED VOLTAGE VECTOR IS LOCATED

Desired voltage vector sector					
1	2	3	4	5	6
v_1	v_2	v_3	v_4	v_5	v_6

TABLE III
CANDIDATE ACTIVE VECTORS BASED ON INPUT VOLTAGE SECTOR AND PROPER DIRECTION OF VECTORS

	Input voltage sector					
	1	2	3	4	5	6
v_1	+1, +2, −3	−1, +2, −3	−1, +2, +3	−1, −2, +3	+1, −2, +3	+1, −2, −3
v_2	−7, −8, +9	+7, −8, +9	+7, −8, −9	+7, +8, −9	−7, +8, −9	−7, +8, −9
v_3	+4, +5, −6	−4, +5, −6	−4, +5, +6	−4, −5, +6	+4, −5, +6	+4, −5, −6
v_4	−1, −2, +3	+1, −2, +3	+1, −2, −3	+1, +2, −3	−1, +2, −3	−1, +2, −3
v_5	+7, +8, −9	−7, +8, −9	−7, +8, +9	−7, −8, +9	+7, −8, +9	+7, −8, −9
v_6	−4, −5, +6	+4, −5, +6	+4, −5, −6	+4, +5, −6	−4, +5, −6	−4, +5, +6

C. Overall Control Procedure

The proposed simplified FCS-MPC for matrix converter-fed PMSM includes four main parts:

1) calculation of the desired voltage vector and the sector which is located;
2) determining the candidate vectors for prediction;
3) prediction of input reactive power;
4) minimization of the cost function.

The desired voltage vector is calculated by (15) and the sector which is located is determined according to (18). A Lookup table is used to determine the closest direction of active vectors to the desired voltage vector, based on the location of the desired voltage vector, as presented in Table II. A second lookup table, see Table III, is used to determine the three active vectors of matrix converter based on Table II, and the sector that input voltage vector is located. The input reactive power is predicted for the three active vectors and six rotating vectors and one zero

TABLE IV
SYSTEM PARAMETERS

Parameter	Description	Value
p	Number of pole pairs	4
R_s (Ω)	Stator resistance	0.7
L_s (mH)	Stator inductance	8
φ_m (mWb)	Rotor magnet flux	0.14
v_{rms} (V)	Source line to line voltage	220
ω_r (r/min)	Rated speed	2000
T_r (Nm)	Rated torque	4.7
L_f (mH)	Input filter inductance	0.8
C_f (μF)	Input filter capacitance	30

vector. The cost function (17) is used for evaluating these ten vectors and selecting the best one for actuation.

Considering the delay compensation technique suggested in [38], the overall process of the proposed simplified FCS-MPC for a matrix converter-fed PMSM can be summarized as following steps:

Step 1: Measuring currents, voltages, and speed.
Step 2: Actuating the optimal switching state decided in previous control interval.
Step 3: Predicting the stator current and the input current for the actuated switching state.
Step 4: Determining the desired voltage vector using (15).
Step 5: Selecting three active vectors through lookup Tables II and III.
Step 6: Predicting the input reactive power for the three active vectors, six rotating vectors, and a zero vector using (12) and (13).
Step 7: Evaluating the cost function (17) and determining the optimal switching state.

V. EXPERIMENTAL RESULTS

The proposed simplified FCS-MPC method has been implemented experimentally for a matrix converter-fed 1-kW PMSM and its performance is evaluated and compared with the conventional FCS-MPC method.

The matrix involves 18 insulated-gate bipolar transistors (IXDN 25N120D1) in common emitter configuration. The matrix converter has been connected to the grid voltage through a variac and an input *LC* filter. A protection clamp circuit has been paralleled with the matrix converter. This clamp circuit consists of input and output diode bridges with 12 fast-recovery diodes, an electrolytic capacitor, and a resistor to discharge the capacitor. An induction machine driven by a Danfoss VLT FC-302 3.0 kW inverter has been used as a load for PMSM. The parameters of the PMSM and input filter are listed in Table IV.

The control algorithms have been implemented in C code by using a digital signal processor (DSP) model TMS320F2812.

The results are presented for three algorithms including conventional FCS-MPC, simplified FCS-MPC with evaluation of 25 switching states, and further simplified FCS-MPC with evaluation of ten switching states.

A. Investigation of Dynamic Behavior

The dynamic behavior of the system during a speed reversal, where the reference speed changes from 2000 to -2000 r/min, is shown in Figs. 3, 4, and 5, for conventional FCS-MPC, simplified FCS-MPC, and further simplified FCS-MPC, respectively. These experimentations show performances of the methods at different operating points. The sampling time for the three methods is $T_s = 60\,\mu$s. The reference of input reactive power Q^* in the cost functions (14) and (17) is set to 0 to have a unity power factor in the input side. It can be observed that all the three methods have good performances regarding the input and output side control objectives. The methods present smooth tracking of reference speed and sinusoidal motor current with its frequency being proportional to the rotor speed. Regarding the input side, in the all three methods the input current has a sinusoidal waveform which is achieved by the control of the input reactive power. It can be observed that the source current is in phase with the source voltage for the duration of motoring operation. However, reduction of the speed during the speed reversal decreases the kinetic energy and demands the drive to regenerate energy. In this case, sinusoidal input currents with π rad phase shift with the phase voltage causes the energy flows from the motor to the source (regenerating mode).

B. Investigation of Steady-State Behavior

The steady-state performances of the system with conventional algorithm and the proposed simplified algorithms are investigated and the results are presented in Fig. 6. For the all three methods, the motor operates at rated speed (2000 r/min) with a full load (4.7 Nm) and the sampling time is $T_s = 60\,\mu$s. It is shown that the methods work very well and accomplish smooth speed and sinusoidal motor current. The total harmonic distortion (THD) of motor current is 1.82% for conventional FCS-MPC and it is 1.81% and 1.86% for the simplified FCS-MPC and further simplified FCS-MPC methods, respectively. Concerning the input side variables, as a result of reactive power control with $Q^* = 0$ in the cost functions, the input reactive power is close to zero and the input current has sinusoidal wave form with low ripple and is synchronized with the related source phase voltage, resulting in unity power factor. The THD of input current is 4.54% for conventional FCS-MPC and it is 4.7% and 5.5% for the simplified FCS-MPC and further simplified FCS-MPC methods.

It is worth mentioning that the running time for execution of each algorithm is different. The average execution times of the three algorithms are presented and compared in Table V. In the simplified FCS-MPC, 25 calculations of current prediction are avoided in comparison with conventional FCS-MPC. So, the execution time is reduced considerably. In further simplified FCS-MPC, with reducing candidate switching states for prediction and evaluation in the cost function, from 25 to 10, the execution time of the algorithm is reduced more. It should be noted that the election of candidate switching states requires extra calculations. However, the required time for these calculations is much less than the time decreased in the prediction and evaluation steps.

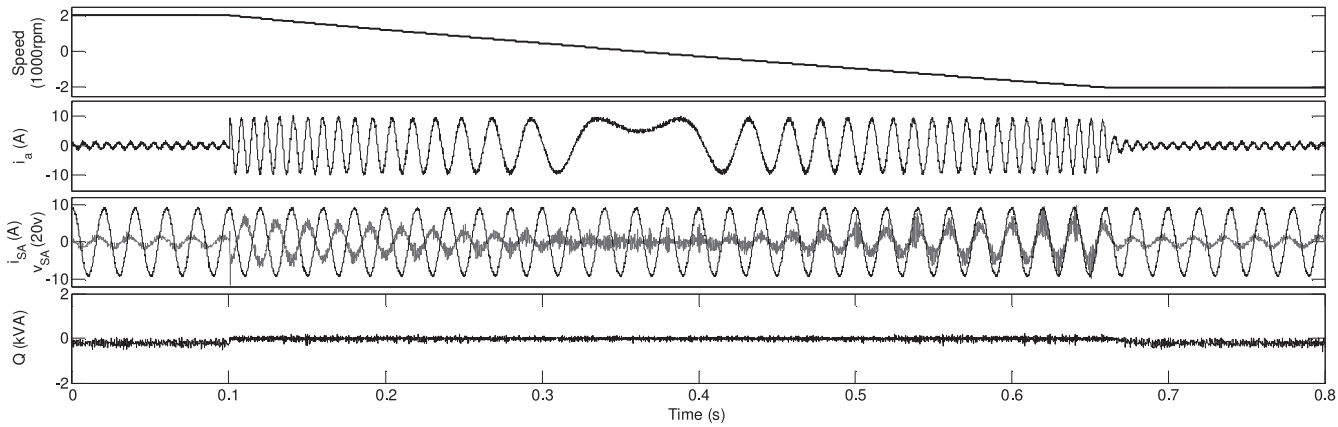

Fig. 3. Experimental performance of the conventional FCS-MPC during a full-speed reversal maneuver.

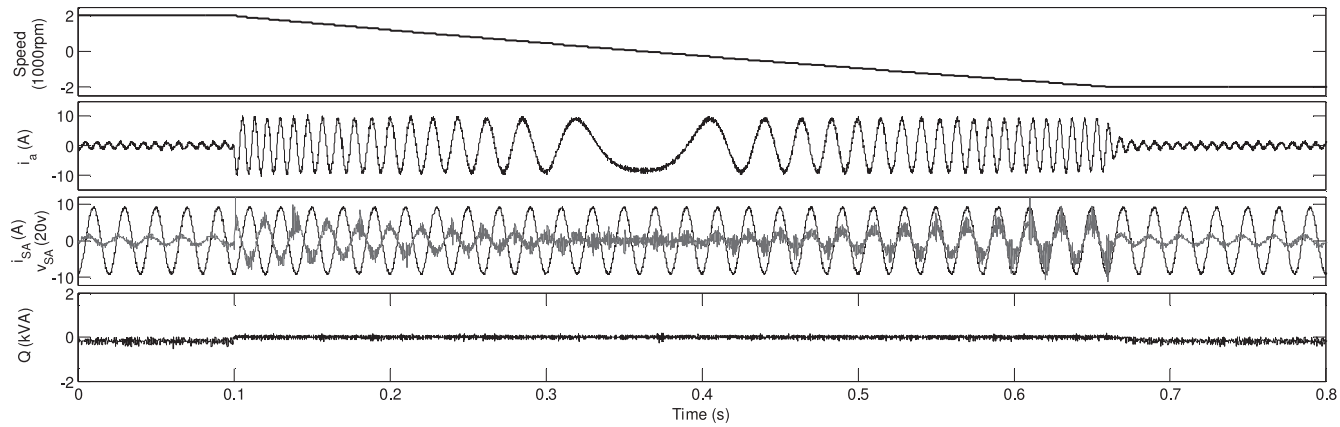

Fig. 4. Experimental performance of the simplified FCS-MPC with evaluation of 25 switching states during a full-speed reversal maneuver.

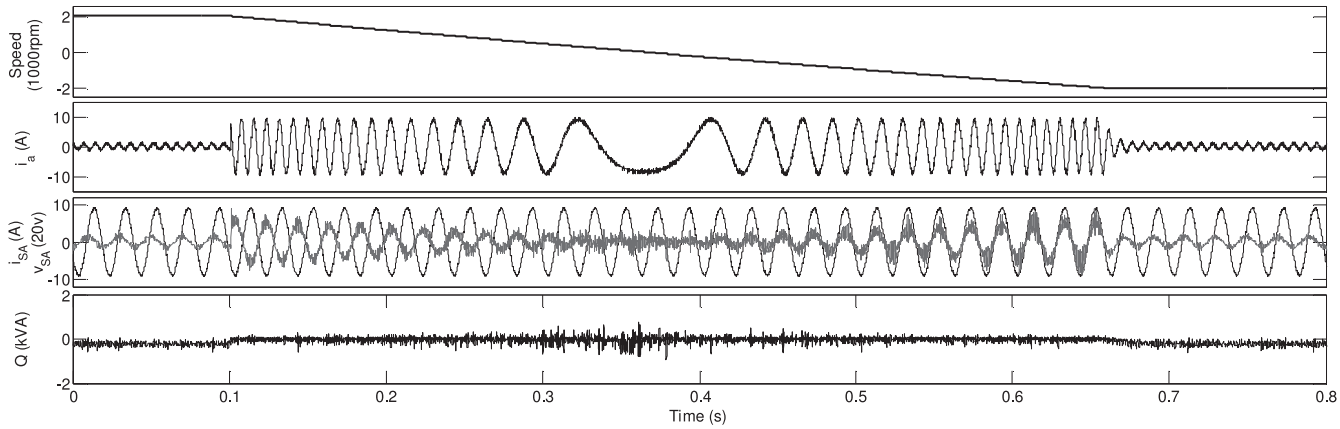

Fig. 5. Experimental performance of the further simplified FCS-MPC with evaluation of ten switching states during a full-speed reversal maneuver.

Considering the required execution time, the sampling time for conventional FCS-MPC cannot be much less than 60 μs. But, it is possible to reduce the sampling time for simplified FCS-MPC algorithms. The sampling time can be set to 48 μs for simplified FCS-MPC with evaluation of 25 switching states and it can be set to 28 μs when only 10 switching states are evaluated. The steady-state performances of the system for simplified FCS-MPC with $T_s = 48\,\mu$s and for further simplified FCS-MPC with $T_s = 28\,\mu$s are presented in Figs. 7 and 8, respectively. The THD of stator current is 1.6% and 0.9% for Figs. 7 and 8, respectively. The THD of input current is 3.15% and 2.86% for Figs. 7 and 8, respectively.

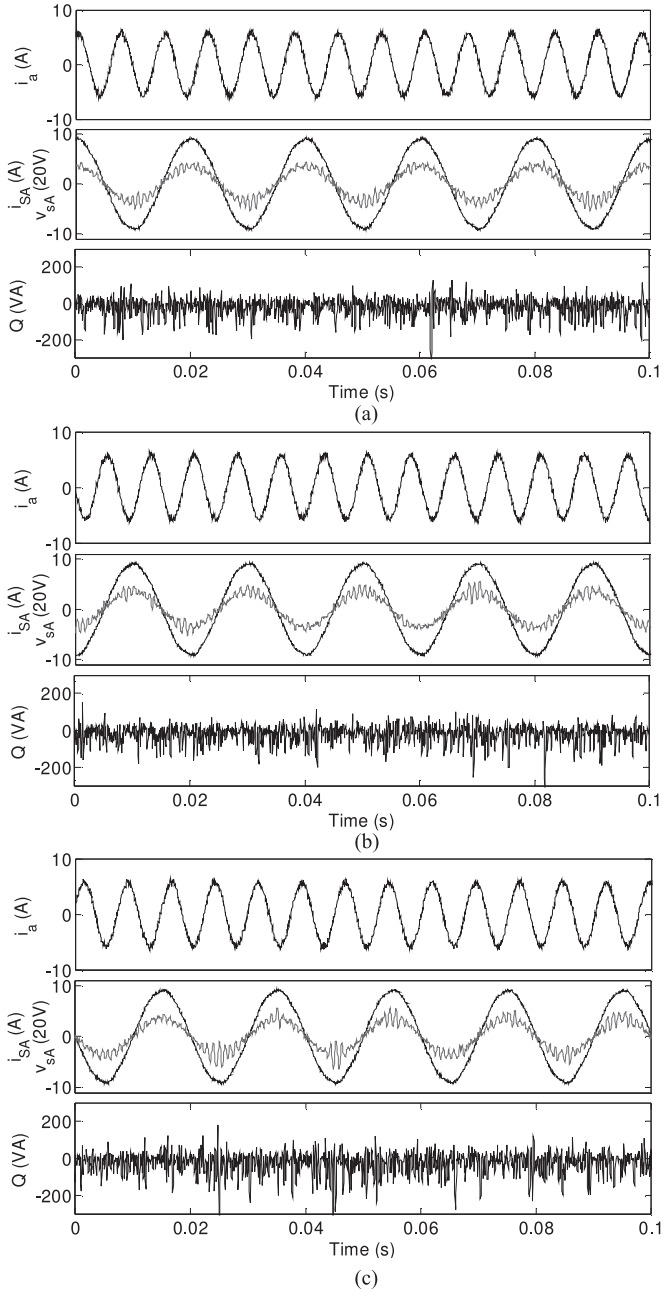

Fig. 6. Experimental steady-state performance of the system with $T_s = 60\,\mu$s. (a) Conventional FCS-MPC, (b) simplified FCS-MPC, and (c) further simplified FCS-MPC.

TABLE V
COMPARISON OF AVERAGE EXECUTION TIMES OF THE CONVENTIONAL FCS-MPC AND SIMPLIFIED FCS-MPC

Task	Execution Time (μs)		
	Conventional FCS-MPC	Simplified FCS-MPC	Further simplified FCS-MPC
Measurement and initial calculations	6.09	6.4	6.4
Selection of candidate switching states	0	0	2.65
Prediction and evaluation	50.2	37.46	14.55
Total	56.29	43.86	23.6

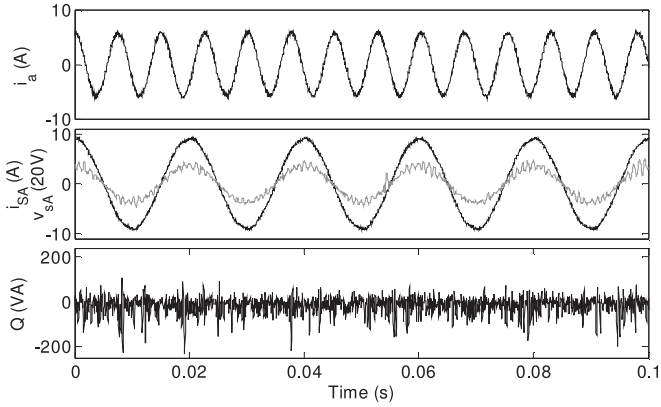

Fig. 7. Experimental steady-state performance of the simplified FCS-MPC with $T_s = 48\,\mu$s.

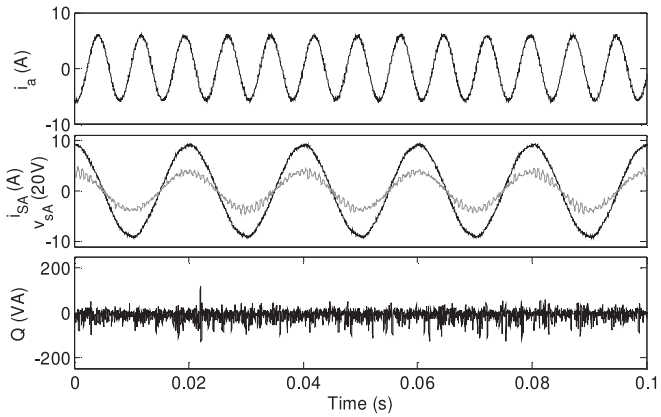

Fig. 8. Experimental steady-state performance of the further simplified FCS-MPC with $T_s = 28\,\mu$s.

TABLE VI
AVERAGE SWITCHING FREQUENCY FOR FIGS. 6–8

Sampling Time (μs)	Average Switching Frequency (kHz)		
	Conventional FCS-MPC	Simplified FCS-MPC	Further simplified FCS-MPC
60	1.61	1.61	1.6
48	–	1.96	–
28	–	–	3.18

C. Investigation of Switching Frequency

The average switching frequencies for Figs. 6–8 have been presented in Table VI. It is should be noted that in these tests there is no switching frequency penalization term in the corresponding cost function. It is seen that for $T_s = 60\,\mu$s the average switching frequencies are similar for conventional and the simplified FCS-MPC with evaluation of 25 switching states; however, the average switching frequency is bit higher for the further simplified FCS-MPC with evaluation of 10 switching states. Reducing the sampling time for the proposed simplified

TABLE VII
MEASURED RESULTS WITH AND WITHOUT PENALIZING SWITCHING FREQUENCY

Sample time (μs)	Variable	Conventional FCS-MPC		Simplified FCS-MPC		Further simplified FCS-MPC	
		$k_{\rm sw}$					
		0	0.19	0	24	0	38
65	*THD_i*$_o$ (%)	1.91	1.97	1.91	1.98	2.04	2.1
	THD_i$_s$ (%)	4.79	5.75	4.8	5.74	6.1	7.17
	Switching frequency (*kHz*)	1.48	1.26	1.49	1.27	1.46	1.27
53	*THD_i*$_o$ (%)	–	–	1.78	1.86	–	–
	THD_i$_s$ (%)	–	–	3.33	3.83	–	–
	Switching frequency (*kHz*)	–	–	1.8	1.53	–	–
30	*THD_i*$_o$ (%)	–	–	–	–	0.93	0.97
	THD_i$_s$ (%)	–	–	–	–	2.9	3.28
	Switching frequency (*kHz*)	–	–	–	–	2.96	2.4

methods results in increase of average switching frequencies of these methods, as presented in Table VI.

As mentioned previously, for Figs. 6–8, the switching frequency reduction was not considered in the algorithms.

However, this goal can be easily achieved in FCS-MPC by assigning a cost to switching states that involve a higher number of commutations [39], [40]. For this purpose, the cost functions (14) and (17), respectively, change to

$$\mathrm{CF}_{\rm sw} = \left|\mathbf{i}_o^*(k) - \mathbf{i}_{o|\rm sw}\right| + k_Q\,|Q^* - Q_{\rm sw}(k+1)| + k_{\rm sf}\cdot n_{\rm sw} \tag{19}$$

$$\mathrm{CF}_{\rm sw} = \left|\mathbf{v}_o^*(k) - \mathbf{v}_{o|\rm sw}\right| + k_Q\,|Q^* - Q_{\rm sw}(k+1)| + k_{\rm sf}\cdot n_{\rm sw} \tag{20}$$

where n is the number of commutations imposed by the switching state under evaluation (sw), and $k_{\rm sf}$ is a weighting factor. The calculation of the number of commutations in the application of each switching state is easy and straightforward. The number of the commutations can be simply determined through a table containing the value of n (number of commutations) between each combination of the possible switching states of the matrix converter. The rows of this table denote the switching state under evaluation and the columns denote the previous switching state. Thus, implementation of this procedure in a DSP is very easy. It is worth mentioning that these calculations increase the execution time of the algorithms to 60.92, 48.48, and 25.51 μs for conventional FCS-MPC, simplified FCS-MPC, and further simplified FCS-MPC. Therefore, setting the sampling time to 65 μs provides enough time for completing the conventional FCS-MPC algorithm. However, it is possible to set shorter sampling times of 53 and 30 μs for the simplified FCS-MPC and further simplified FSC-MPC. A summary of measured results has been presented in Table VII. It is possible to observe that penalizing the switching frequency in the cost functions achieves lower switching frequencies, but, presents a higher amount distortion in motor and source currents.

VI. CONCLUSION

A simplified FCS-MPC method for a matrix converter-fed PMSM has been proposed in this paper to reduce the calculations efforts imposed by the conventional FCS-MPC. This simplification is done through two main changes in conventional FCS-MPC: 1) avoiding motor current predictions: and 2) reducing the candidate switching states for prediction and evaluation. The first change helps the method to skip the 25 current predictions and the second change reduces the 25 predictions of reactive power and 25 evaluations of the cost function to 10 predictions of reactive power and 10 evaluations of the cost function. It has been shown through the experimental tests that the proposed approach can significantly reduce the execution time of the FCS-MPC algorithm, while the performance of the proposed simplified FCS-MPC is very similar to conventional FCS-MPC. Furthermore, the lower execution time makes it possible to reduce the sampling time which improves the behavior of the control objectives, i.e., a lower THD for stator current and input current.

ACKNOWLEDGMENT

The Authors acknowledge the Center of Excellence for Power Systems Automation and Operation, Department of Electrical Engineering, Iran University of Science and Technology.

REFERENCES

[1] T. Friedli, J. W. Kolar, J. Rodriguez, and P. W. Wheeler, "Comparative evaluation of three-phase ac–ac matrix converter and voltage dc-link back-to-back converter systems," *IEEE Trans. Ind. Electron.*, vol. 59, no. 12, pp. 4487–4510, Dec. 2012.

[2] A. Alesina and M. Venturini, "Solid-state power conversion: A Fourier analysis approach to generalized transformer synthesis," *IEEE Trans. Circuits Syst.*, vol. CAS-28, no. 4, pp. 319–330, Apr. 1981.

[3] J. Rodriguez, M. Rivera, J. Kolar, and P. Wheeler, "A review of control and modulation methods for matrix converters," *IEEE Trans. Ind. Electron.*, vol. 59, no. 1, pp. 58–70, Jan. 2012.

[4] J. Rodríguez *et al.*, "State of the art of finite control set model predictive control in power electronics," *IEEE Trans. Ind. Informat.*, vol. 9, no. 2, pp. 1003–1016, May 2013.

[5] M. Siami, D. A. Khaburi, A. Abbaszadeh, and J. Rodríguez, "Robustness improvement of predictive current control using prediction error correction for permanent-magnet synchronous machines," *IEEE Trans. Ind. Electron.*, vol. 63, no. 6, pp. 3458–3466, Jun. 2016.

[6] G. A. Papafotiou, G. D. Demetriades, and V. G. Agelidis, "Technology readiness assessment of model predictive control in medium–and high-voltage power electronics," *IEEE Trans. Ind. Electron.*, vol. 63, no. 9, pp. 5807–5815, Sep. 2016.

[7] M. Siami, D. A. Khaburi, and J. Rodríguez, "Torque ripple reduction of predictive torque control for PMSM drives with parameter mismatch," *IEEE Trans. Power Electron.*, vol. 32, no. 9, pp. 7160–7168, Sep. 2017.

[8] S. Vazquez, J. Rodriguez, M. Rivera, L. G. Franquelo, and M. Norambuena, "Model predictive control for power converters and drives: Advances and trends," *IEEE Trans. Ind. Electron.*, vol. 64, no. 2, pp. 935–947, Feb. 2017. Doi: 10.1109/TIE.2016.2625238

[9] M. Siami, S. A. Gholamian, and M. Yousefi, "A comparative study between direct torque control and predictive torque control for axial flux permanent magnet synchronous machines," *J. Electr. Eng.*, vol. 64, no. 6, pp. 346–353, Dec. 2013.

[10] J. Holtz, "Advanced PWM and predictive control—An overview," *IEEE Trans. Ind. Electron.*, vol. 63, no. 6, pp. 3837–3844, Jun. 2016.

[11] R. P. Aguilera, P. Lezana, and D. E. Quevedo, "Finite-control-set model predictive control with improved steady-state performance," *IEEE Trans. Ind. Informat.*, vol. 9, no. 2, pp. 658–667, May 2013.

[12] A. Formentini, A. Trentin, M. Marchesoni, P. Zanchetta, and P. Wheeler, "Speed finite control set model predictive control of a PMSM fed by matrix converter," *IEEE Trans. Ind. Electron.*, vol. 62, no. 11, pp. 6786–6796, Nov. 2015.
[13] R. Vargas, J. Rodriguez, U. Ammann, and P. Wheeler, "Predictive current control of an induction machine fed by a matrix converter with reactive power control," *IEEE Trans. Ind. Electron.*, vol. 55, no. 12, pp. 4362–4371, Dec. 2008.
[14] R. Vargas, U. Ammann, and J. Rodriguez, "Predictive approach to increase efficiency and reduce switching losses on matrix converters," *IEEE Trans. Power Electron.*, vol. 24, no. 4, pp. 894–902, Apr. 2009.
[15] M. Rivera, J. Rodriguez, J. Espinoza, and H. Abu-Rub, "Instantaneous reactive power minimization and current control for an indirect matrix converter under a distorted ac-supply," *IEEE Trans. Ind. Informat.*, vol. 8, no. 3, pp. 482–490, Aug. 2012.
[16] S. Muller, U. Ammann, and S. Rees, "New time-discrete modulation scheme for matrix converters," *IEEE Trans. Ind. Electron.*, vol. 52, no. 6, pp. 1607–1615, Dec. 2005.
[17] M. Rivera, J. Rodriguez, P. Wheeler, C. Rojas, A. Wilson, and J. Espinoza, "Control of a matrix converter with imposed sinusoidal source currents," *IEEE Trans. Ind. Electron.*, vol. 59, no. 4, pp. 1939–1949, Apr. 2012.
[18] M. Rivera *et al.*, "A comparative assessment of model predictive current control and space vector modulation in a direct matrix converter," *IEEE Trans. Ind. Electron.*, vol. 60, no. 2, pp. 578–588, Feb. 2013.
[19] R. Vargas, U. Ammann, B. Hudoffsky, J. Rodriguez, and P. Wheeler, "Predictive torque control of an induction machine fed by a matrix converter with reactive input power control," *IEEE Trans. Power Electron.*, vol. 25, no. 6, pp. 1426–1438, Jun. 2010.
[20] J. Lei *et al.*, "Predictive power control of matrix converter with active damping function," *IEEE Trans. Ind. Electron.*, vol. 63, no. 7, pp. 4550–4559, Jul. 2016.
[21] J. Lei, B. Zhou, X. Qin, J. Wei, and J. Bian, "Active damping control strategy of matrix converter via modifying input reference currents," *IEEE Trans. Power Electron.*, vol. 30, no. 9, pp. 5260–5271, Sep. 2015.
[22] T. Geyer, "Computationally efficient model predictive direct torque control," *IEEE Trans. Power Electron.*, vol. 26, no. 10, pp. 2804–2816, Oct. 2011.
[23] T. Geyer and D. E. Quevedo, "Multistep finite control set model predictive control for power electronics," *IEEE Trans. Power Electron.*, vol. 29, no. 12, pp. 6836–6846, Dec. 2014.
[24] B. Stellato, T. Geyer, and P. J. Goulart, "High-speed finite control set model predictive control for power electronics," *IEEE Trans. Power Electron.*, vol. 32, no. 5, pp. 4007–4020, May 2017.
[25] Y. L. Zhang and H. Lin, "Simplified model predictive current control method of voltage-source inverter," in *Proc. 8th Int. Conf. Power Electron. ECCE Asia*, 2011, pp. 1726–1733.
[26] Y. Zhang, W. Xie, Z. Li, and Y. Zhang, "Low-complexity model predictive power control: Double-vector- based approach," *IEEE Trans. Ind. Electron.*, vol. 61, no. 11, pp. 5871–5880, Nov. 2014.
[27] P. Cortes, A. Wilson, S. Kouro, J. Rodriguez, and H. Abu-Rub, "Model predictive control of multilevel cascaded H-bridge inverters," *IEEE Trans. Ind. Electron.*, vol. 57, no. 8, pp. 2691–2699, Aug. 2010.
[28] J. Hu, J. Zhu, G. Lei, G. Platt, and D. G. Dorrell, "Multi-objective model-predictive control for high-power converters," *IEEE Trans. Energy Convers.*, vol. 28, no. 3, pp. 652–663, Sep. 2013.
[29] A. Iqbal, H. Abu-Rub, S. K. M. Ahmed, P. Cortes, and J. Rodriguez, "Model predictive current control o f a three-level five-phase NPC VSI using simplified computational approach," in *Proc. 29th Annu. IEEE Appl. Power Electron. Conf. Expo.*, Mar. 2014, pp. 2323–2330.
[30] M. Habibullah, D. D. C. Lu, D. Xiao, and M. F. Rahman, "A simplified finite-state predictive direct torque control for induction motor drive," *IEEE Trans. Ind. Electron.*, vol. 63, no. 6, pp. 3964–3975, Jun. 2016.
[31] M. Siami, D. Arab Khaburi, M. Rivera, and J. Rodriguez, "A computationally efficient lookup table based FCS-MPC for PMSM drives fed by matrix converters," in *IEEE Trans. Ind. Electron.*, 2017, to be published. Doi: 10.1109/TIE.2017.2694392
[32] C. Xia, T. Liu, T. Shi, and Z. Song, "A simplified finite-control-set model-predictive control for power converters," *IEEE Trans. Ind. Informat.*, vol. 10, no. 2, pp. 991–1002, May 2014.
[33] W. Xie *et al.*, "Finite-control-set model predictive torque control with a deadbeat solution for PMSM drives," *IEEE Trans. Ind. Electron.*, vol. 62, no. 9, pp. 5402–5410, Sep. 2015.
[34] Y. Zhang and W. Xie, "Low complexity model predictive control—Single vector-based approach," *IEEE Trans. Power Electron.*, vol. 29, no. 10, pp. 5532–5541, Oct. 2014.
[35] M. Siami, H. K. Savadkoohi, A. Abbaszadeh, D. A. Khaburi, J. Rodriguez, and M. Rivera, "Predictive torque control of a permanent magnet synchronous motor fed by a matrix converter without weighting factor," in *Proc. 2016 7th Power Electron. Drive Syst. Technol. Conf.*, Tehran, 2016, pp. 614–619.
[36] C. A. Rojas, J. Rodríguez, F. Villarroel, J. R. Espinoza, C. A. Silva, and M Trincado, "Predictive torque and flux control without weighting factors," *IEEE Trans. Ind. Electron.*, vol. 60, no. 2, pp. 681–690, Feb. 2013.
[37] C. Ortega, A. Arias, C. Caruana, J. Balcells, and G. M. Asher, "Improved waveform quality in the direct torque control of matrix-converter-fed PMSM drives," *IEEE Trans. Power Electron.*, vol. 57, no. 6, pp. 2101–2110, Jun. 2010.
[38] P. Cortes, J. Rodriguez, C. Silva, and A. Flores, "Delay compensation in model predictive current control of a three-phase inverter," *IEEE Trans. Ind. Electron.*, vol. 59, no. 2, pp. 1323–1325, Feb. 2012.
[39] R. Vargas, P. Cortes, U. Ammann, J. Rodriguez, and J. Pontt, "Predictive control of a three-phase neutral-point-clamped inverter," *IEEE Trans. Ind. Electron.*, vol. 54, no. 5, pp. 2697–2705, Oct. 2007.
[40] R. Vargas, U. Ammann, and J. Rodriguez, "Predictive approach to increase efficiency and reduce switching losses on matrix converters," *IEEE Trans. Power Electron.*, vol. 24, no. 4, pp. 894–902, Apr. 2009.

Mohsen Siami was born in Mazandaran, Iran, in 1986. He received the B.Sc. degree from Guilan University, Rasht, Iran, in 2009, and the M.S. degree from the Babol (Noshirvani) University of Technology, Babol, Iran, in 2012, both in electrical engineering. He is currently working toward the Ph.D. degree in electrical engineering at the Iran University of Science and Technology (IUST), Tehran, Iran.

Since 2013, he has been a Lecturer with IUST. His researh intrests include predictive control, robust control, and matrix converter.

Davood Arab Khaburi was born in 1965. He has received the B.Sc. degree in electronic engineering, in 1990, from the Sharif University of Technology, Tehran, Iran, and the M.Sc. and Ph.D. degrees in electrical engineering from ENSEM, INPEL, Nancy, France, in 1994 and 1998, respectively.

He has joined the University of Technology of Compiègne, Compiegne, France, for one year (1998–1999). Since January of 2000, he has been as a faculty member in the Electrical Engineering Department, Iran University of Science Technology (IUST), Tehran, Iran, where he is currently an Associate Professor. He is one of the founders of the Iranian Association of Power Electronics, and currently a board member of this association. He is also a member of the Center of Excellence for Power Systems Automation and Operation. Currently, he is the Head of power group at IUST. His research interests include power electronics, motor drives, and digital control.

Jose Rodriguez (M'81–SM'94–F'10) received the Engineer degree from the Universidad Tecnica Federico Santa Maria, Valparaiso, Chile, in 1977, and the Dr.-Ing. degree from the University of Erlangen, Erlangen, Germany, in 1985, both in electrical engineering.

Since 1977, he has been in the Department of Electronics Engineering, Universidad Tecnica Federico Santa Maria, where he was a Full Professor and the President. Since 2015, he has been the President of the Universidad Andres Bello, Santiago, Chile. He has coauthored two books, several book chapters, and more than 400 journal and conference papers. His main research interests include multilevel inverters, new converter topologies, control of power converters, and adjustable-speed drives.

Dr. Rodriguez is a member of the Chilean Academy of Engineering. He received a number of best paper awards from journals of the IEEE, the National Award of Applied Sciences and Technology from the government of Chile in 2014, and the Eugene Mittelmann Award from the Industrial Electronics Society of the IEEE in 2015.